Orthotropic elastic shell model for buckling of microtubules

C. Y. Wang, C. Q. Ru,* and A. Mioduchowski
Department of Mechanical Engineering, University of Alberta, Edmonton, Canada T6G 2G8
(Received 26 April 2006; revised manuscript received 7 September 2006; published 14 November 2006)

In view of the fact that microtubules exhibit strong anisotropic elastic properties, an orthotropic elastic shell model for microtubules is developed to study buckling behavior of microtubules. The predicted critical pressure is found to agree well with recent unexplained experimental data on pressure-induced buckling of microtubules [Needleman *et al.*, Phys. Rev. Lett. **93**, 198104 (2004); Biophys. J. **89**, 3410 (2005)] which are lower than that predicted by the isotropic shell model by four orders of magnitude. General buckling behavior of microtubules under axial compression or radial pressure is studied. The results show that the isotropic shell model greatly overestimates the bucking loads of microtubules, except columnlike axially compressed buckling of long microtubules (of length-to-diameter ratio larger than, say, 150). In particular, the present results also offer a plausible explanation for the length dependency of flexibility of microtubules reported in the literature.

DOI: 10.1103/PhysRevE.74.052901 PACS number(s): 87.16.Ka, 87.15.La

Microtubules (MTs) are the most rigid filaments of eukaryotic cytoskeleton and largely responsible for shape and mechanical rigidity of cells [1,2]. In shape, MTs are long hollow cylinders with outer and inner diameters of about 30 and 20 nm, respectively. MT mechanics has been the topic of numerous recent theoretical and experimental researches, including those on elastic buckling [3–9] and force-related morphological instability [10–13]. For example, pressure-induced buckling of hollow MTs has been observed in Refs. [8,9], and a theoretical estimate of the critical pressure based on isotropic homogeneous elastic shell model is found to be higher than the experimental value by four orders of magnitude.

Besides various discrete methods of modeling, simple continuum elastic beam models have been effectively used to study one-dimensional (1D) rodlike mechanical behavior of MTs, such as flexural rigidity of MTs [14–18], and rodlike buckling [3–6]. In addition, an isotropic elastic shell model has been developed earlier in Ref. [19] to study free vibration of MTs. However, recent experiments have confirmed that the longitudinal bonds between $\alpha\beta$-tubulin dimers along protofilaments are much stronger than the lateral bonds between adjacent protofilaments [9,20,21]. In particular, shear modulus of MTs is much lower than the longitudinal elastic modulus, and the circumferential elastic modulus is lower than the longitudinal elastic modulus by a few orders of magnitude [22–24]. In addition, the molecular mechanics model shows [12] that small helix of MTs is less relevant for mechanical behavior of MTs. These results suggest that MTs could be modeled as an orthotropic elastic shell with independent longitudinal modulus, circumferential modulus, and shear modulus. Inspired by valid application of elastic shell models to carbon nanotubes [25–27], a simple orthotropic elastic shell model is suggested in the present paper. Since an orthotropic shell has four independent material constants (including longitudinal modulus E_x, circumferential modulus E_θ, shear modulus $G_{x\theta}$, and Poisson ratio ν_x along the longitudinal direction) [28,29], the range of the values of these material constants for MTs are identified from the date available in the literature, and summarized in Table I. In particular, following the literature, the cross section of MTs will be treated as an equivalent circular annular shape, with an equivalent thickness $h \approx 2.7$ nm (see, e.g., Refs. [7,19]). Thus all elastic moduli, in-plane stiffnesses, and the mass density ρ are defined based on such a thickness $h=2.7$ nm.

On the other hand, the bending stiffness of MTs is determined largely by a so-called "bridge" thickness of MTs (of 1.1 nm, see Fig. 2 of Ref. [7]) which is much smaller than $h=2.7$ nm. Thus similar as single-walled carbon nanotubes [25–27,30,31], the effective bending stiffness of MTs, modeled as an elastic shell, should be considered to be an independent material constant. According to experimental data on shell-like buckling of individual MTs, the bending stiffness of MTs can be estimated by an effective thickness determined in Ref. [7], which is about 1.6 nm. For example, if the longitudinal modulus $E_x=1$ GPa, the effective bending stiffness along the longitudinal direction D_x is given by $D_x = \frac{E_x h_0^3}{12(1-\nu_x \nu_\theta)}$ with the effective thickness $h_0=1.6$ nm, which is about 3.42×10^{-19} Nm.

Thus modeled as an orthotropic elastic shell, buckling of an individual MT under axial and circumferential prestresses N_x and N_θ (the former is generated by uniform axial compressive force, while the latter is generated by uniform external radial pressure) are governed by three equilibrium equations [32–35],

TABLE I. The values of orthotropic material constants for microtubules.

Parameters		Values	References
Longitudinal modulus	E_x	0.5–2 GPa	[7,19,24]
Circumferential modulus	E_θ	1–4 MPa	[24]
Shear modulus in x-θ plane	$G_{x\theta}$	~1 MPa	[7,22–24]
Poisson's ratio in axial direction	ν_x	0.3	[19,24]
Mass density per unit volume	ρ	1.47 g/cm^3	[19]
Equivalent thickness	h	2.7 nm	[7,19]
Effective thickness for bending	h_0	1.6 nm	[7]

*Corresponding author. Electronic address: c.ru@ualberta.ca

$$\begin{Bmatrix} (K_x+N_x)R^2\dfrac{\partial^2}{\partial x^2} \\ +\left(\dfrac{K_{x\theta}R^2+D_{x\theta}}{R^2}+N_\theta\right)\dfrac{\partial^2}{\partial\theta^2} \end{Bmatrix} u + \left\{R(\nu_x K_\theta + K_{x\theta})\frac{\partial^2}{\partial x\,\partial\,\theta}\right\} v + \begin{Bmatrix} -R(\nu_\theta K_x - N_\theta)\dfrac{\partial}{\partial x} \\ +RD_x\dfrac{\partial^3}{\partial x^3} \\ -\dfrac{D_{x\theta}}{R}\dfrac{\partial^3}{\partial x\,\partial\,\theta^2} \end{Bmatrix} w = 0,$$

$$\left\{R(\nu_\theta K_x + K_{x\theta})\frac{\partial^2}{\partial x\,\partial\,\theta}\right\} u + \begin{Bmatrix} (K_\theta+N_\theta)\dfrac{\partial^2}{\partial\theta^2} \\ +\left(\dfrac{K_{x\theta}R^2+3D_{x\theta}}{R^2}+N_x\right)R^2\dfrac{\partial^2}{\partial x^2} \end{Bmatrix} v + \begin{Bmatrix} -(K_\theta+N_\theta)\dfrac{\partial}{\partial\theta} \\ +(\nu_\theta D_x+3D_{x\theta})\dfrac{\partial^3}{\partial x^2\,\partial\,\theta} \end{Bmatrix} w = 0,$$

$$\begin{Bmatrix} R(\nu_\theta K_x - N_\theta)\dfrac{\partial}{\partial x} \\ -RD_x\dfrac{\partial^3}{\partial x^3} \\ +\dfrac{D_{x\theta}}{R}\dfrac{\partial^3}{\partial x\,\partial\,\theta^2} \end{Bmatrix} u + \begin{Bmatrix} (K_\theta+N_\theta)\dfrac{\partial}{\partial\theta} \\ -(\nu_\theta D_x+3D_{x\theta})\dfrac{\partial^3}{\partial x^2\,\partial\,\theta} \end{Bmatrix} v + \begin{Bmatrix} -R^2D_x\dfrac{\partial^4}{\partial x^4} \\ -(2\nu_\theta D_x+4D_{x\theta})\dfrac{\partial^4}{\partial x^2\,\partial\,\theta^2} \\ -\dfrac{D_\theta}{R^2}\left(\dfrac{\partial^2}{\partial\theta^2}+1\right)^2 \\ +N_\theta\dfrac{\partial^2}{\partial\theta^2}+N_xR^2\dfrac{\partial^2}{\partial x^2}-K_\theta \end{Bmatrix} w = 0, \quad (1)$$

where x and θ are the axial coordinate and circumferential angular coordinate, respectively, u, v, and w are the axial displacement, circumferential displacement, and radial (inward) deflection, respectively, ρ is the mass density (per unit volume), R is the average radius, and $\gamma=h_0^3/(12hR^2)$. In addition, ν_x and ν_θ are Poisson ratios satisfying $\nu_\theta/\nu_x=E_\theta/E_x$, and $K_x[=E_xh/(1-\nu_x\nu_\theta)]$, $K_\theta[=E_\theta h/(1-\nu_x\nu_\theta)]$, and $K_{x\theta}$ $(=G_{x\theta}h)$ are in-plane stiffnesses in longitudinal and circumferential directions, and in-plane stiffness in shear, respectively, and $D_x[=E_xh_0^3/12(1-\nu_x\nu_\theta)]$, $D_\theta[=E_xh_0^3/12(1-\nu_x\nu_\theta)]$, and $D_{x\theta}(=G_{x\theta}h_0^3/12)$ are the effective bending stiffnesses in longitudinal and circumferential directions, and bending stiffness in shear, respectively [32–35]. Therefore, for given h and h_0, the orthotropic shell model depends on four material constants E_x, E_θ, $G_{x\theta}$, and ν_x given by Table I. In what follows, we define $\alpha=\frac{\nu_\theta}{\nu_x}=\frac{E_\theta}{E_x}=\frac{K_\theta}{K_x}=\frac{D_\theta}{D_x}$ and $\beta=\frac{G_{x\theta}}{E_x}$ $\approx\frac{G_{x\theta}}{E_x}(1-\alpha\nu_x^2)=\frac{D_{x\theta}}{D_x}=\frac{K_{x\theta}}{K_x}$ $(\alpha\cdot\nu_x^2\to 0$ see Table I). Thus the orthotropic model is characterized by four parameters E_x, ν_x, α, and β. In particular, the orthotropic shell model reduces to the isotropic elastic shell model with Poisson ratio ν if $\alpha=1$ and $\beta=(1-\nu)/2$.

Assume that the MT is simply supported at two ends. The buckling mode is given by $u(x,\theta)=U\cos\frac{m\pi}{L}x\cos n\theta$, $v(x,\theta)=V\sin\frac{m\pi}{L}x\sin n\theta$, $w(x,\theta)=W\sin\frac{m\pi}{L}x\cos n\theta$, where U, V, and W are some real constants, n is the circumferential wave number, m is the half axial wave number, L is the length of MT, and the dimensionless axial wavelength (normalized by the diameter $2R$) is calculated as $L/(Rm)$. Substituting them into Eq. (1) yields an eigenequation, and the existence condition of a nonzero solution of (U,V,W) determines buckling load and corresponding buckling mode.

Now, let us first examine buckling of a MT under radial pressure P. In this case, axial prestress $N_x=0$ and circumferential prestress are related to the pressure P by $N_\theta=-PR$. First, let us consider a long MT for which the effect of the end conditions is irrelevant and thus we can seek for axially uniform buckling mode of circumferential wave number $n\geq 2$ [36,37] (as usual, $n=1$ is excluded because it corresponds to a rigid-body translation of circular cross section and does not define buckling under radial pressure). It can be easily verified that when $\frac{\partial}{\partial x}=0$, the three equations in Eq. (1) reduce to a simple equation which gives the lowest critical pressure P_{cr} associated with $n=2$ as

$$P_{cr}=\frac{D_\theta}{R^3}(n^2-1)\approx 3\frac{D_\theta}{R^3}. \quad (2)$$

Thus for $E_\theta=1$ MPa (or $\alpha=E_\theta/E_x=0.001$, see Table I) and $R=13$ nm ($h_0=1.6$ nm), the critical pressure predicted by the above formula is 470 Pa, in good agreement with the experimental value 510–690 Pa reported in Refs. [8,9]. On the other hand, if one takes $E_\theta=4$ MPa and all bending stiffnesses are determined by the so-called "bridge thickness" of 1.1 nm (see Fig. 2 of Ref. [7]), the critical pressure given by Eq. (2) is 600 Pa. Therefore the present orthotropic shell model well explains the experimental value reported in Refs. [8,9] which cannot be explained by the isotropic shell model.

For MTs of typical radius $R=13$ nm, $E_x=1$ GPa, $\nu_x=0.3$, $\alpha=0.001$, and $\beta=0.001$ the critical pressure P_{cr} required for buckling with different $L/(Rm)$ and n is plotted in Fig. 1, with a comparison to the results given by the isotropic shell model (the latter is obtained from the present model by set-

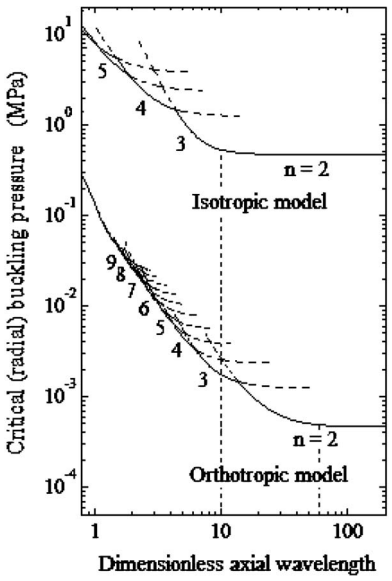

FIG. 1. The dependence of critical (radial) buckling pressure P_{cr} (solid lines) on the dimensionless axial wavelength (normalized by the diameter $2R$) $L/(Rm)$ and n obtained for microtubules of $R=13$ nm, based on the isotropic shell model with $\alpha=1$ and $\beta=0.35$, and the orthotropic shell model with $\alpha=\beta=0.001$.

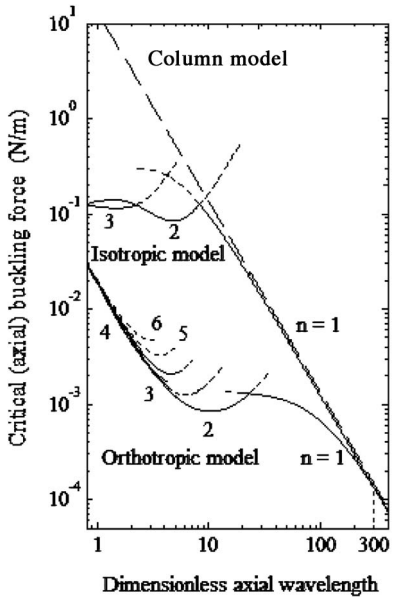

FIG. 2. The dependence of critical (axial) buckling force N_{cr} (solid lines) on the dimensionless axial wavelength (normalized by the diameter $2R$) $L/(Rm)$ and n obtained for microtubules of $R=13$ nm, based on the isotropic shell model with $\alpha=1$ and $\beta=0.35$, and the orthotropic shell model with $\alpha=\beta=0.001$.

ting $\alpha=1$ and $\beta=0.35$). In Fig. 1, the orthotropic shell model predicts that the critical buckling pressure P_{cr} decreases monotonically with increasing $L/(Rm)$ when $L/(Rm)<60$, and then keeps essentially unchanged for $L/(Rm)>60$. This means that for shorter MTs with $L/R<60$, the lowest critical pressure P_{cr} always corresponds to $m=1$. On the other hand, the number n of the corresponding buckling mode decreases as the ratio L/R increases and finally approaches 2 when L/R falls between 20 and 60. On the other hand, for longer MTs of $L/R>60$, as shown in Fig. 1 [also in Eq. (2)], P_{cr}, which is always associated with $n=2$, becomes almost constant and independent of the ratio L/R. In any case, it is clearly seen from Fig. 1 that the isotropic shell model overestimates the critical pressure for buckling of MTs by more than one order of magnitude.

Next, let us examine the buckling of MTs under axial compression and thus $N_\theta=0$. For MTs of typical radius $R=13$ nm, $E_x=1$ GPa, $\nu_x=0.3$, $\alpha=0.001$, and $\beta=0.001$ the critical buckling force N_{cr} required for axially compressed buckling with different $L/(Rm)$ and n is plotted in Fig. 2, with a comparison to the results given by the isotropic shell model and the classical (isotropic) elastic column model (the latter is shown in Fig. 2 by a dashed line). For a sufficiently long MT for which $m=1$ and $n=1$ correspond to the lowest buckling load, it can be verified from Eq. (1) that the critical buckling force given by the present orthotropic shell model is

$$N_{cr}=-\frac{E_x h}{2(1-\nu_x\nu_\theta)}\left(\frac{\pi R}{L}\right)^2\approx-\frac{E_x h}{2}\left(\frac{\pi R}{L}\right)^2.$$

This result is identical to the well-known Euler formula for simply supported columns $F_{cr}=-\frac{\pi^2 E_x I}{L^2}$, showing that the elastic column model agrees well with the orthotropic shell model for axially compressed buckling of very long MTs. Indeed, it is seen from Fig. 2 that the critical length beyond which the elastic column model is accurate is about $L/R=300$, which corresponds to a length of MTs about 4–5 μm. For MTs of length much shorter than 4–5 μm, as shown in Fig. 2, the critical compressive force for buckling given by the elastic column model is much higher than that given by the orthotropic shell model, indicating that the classical elastic column model is inaccurate for shorter MTs. In connection with this, we noticed that flexural rigidity of MTs, estimated based on the elastic column model, have been found to decrease with decreasing length of MTs [17,38] for shorter MTs. The results shown in Fig. 2 suggest that this length dependency of flexural rigidity could be partially attributed to the strong anisotropy of MTs. This issue has been studied recently with more details [39].

In conclusion, a simple orthotropic elastic shell model is developed to study buckling behavior of MTs under axial compression or radial pressure. The critical pressure for buckling of MTs predicted by the present model is in good agreement with recent unexplained experimental data [8,9]. It is believed that the present model offers a simpler approach to study anisotropic shell mechanics of MTs, such as vibration [19,23,24] and dynamic instability [10–13,40,41] of MTs.

The financial support of the Natural Science and Engineering Research Council of Canada (NSERC) is gratefully acknowledged.

[1] J. Howard, *Mechanics of Motor Proteins and the Cytoskeleton* (Sinauer Associates, Inc., Sunderland, 2001).
[2] D. Boal, *Mechanics of the Cell* (Cambridge University Press, Cambridge, England, 2002).
[3] M. Kurachi, M. Hoshi, and H. Tashiro, Cell Motil. Cytoskeleton **30**, 221 (1995).
[4] D. K. Fygenson, J. F. Marko, and A. Libchaber, Phys. Rev. Lett. **79**, 4497 (1997).
[5] D. J. Odde, L. Ma, A. H. Briggs, A. Demarco, and M. W. Kirschner, J. Cell. Sci. **112**, 3283 (1999).
[6] N. Wang, K. Naruse, D. Stamenovic, J. J. Fredberg, S. M. Mijailovich, I. M. Tolic-Norrelykke, T. Polte, R. Mannix, and D. E. Ingber, Proc. Natl. Acad. Sci. U.S.A. **98**, 7765 (2001).
[7] P. J. Pablo, I. A. T. Schaap, F. C. Mackintosh, and C. F. Schmit, Phys. Rev. Lett. **91**, 098101 (2003).
[8] D. J. Needleman, M. A. Ojeda-Lopez, U. R. Kai Ewert, H. P. Miller, L. Wilson, and C. R. Safinya, Biophys. J. **89**, 3410 (2005).
[9] D. J. Needleman, M. A. Ojeda-Lopez, U. Raviv, K. Ewert, J. B. Jones, H. P. Miller, L. Wilson, and C. R. Safinya, Phys. Rev. Lett. **93**, 198104 (2004).
[10] I. M. Janosi, D. Chretien, and H. Flyvbjerg, Biophys. J. **83**, 1317 (2002).
[11] M. E. Janson, M. E. Dood, and M. Dogterom, J. Cell Biol. **161**, 1029 (2003).
[12] M. I. Molodtsov, E. A. Ermakova, E. E. Shnol, E. L. Grishchuk, J. R. McIntosh, and F. I. Ataullakhanov, Biophys. J. **83**, 3167 (2005).
[13] E. L. Grishchuk, M. I. Molodtsov, F. I. Ataulakhanov, and J. R. McLntosh, Nature (London) **438**, 384 (2005).
[14] P. Venier, A. C. Maggs, M. F. Carlier, and J. Pantaloni, Biol. Chem. **269**, 13353 (1994).
[15] F. Gittes, B. Mickey, J. Nettleton, and J. Howard, J. Cell Biol. **120**, 923 (1995).
[16] H. Felgner, R. Frank, and M. Schiwa, J. Cell. Sci. **109**, 509 (1996).
[17] T. Takasone, S. Juodkazis, Y. Kawagishi, A. Yamaguchi, S. Matsuo, H. Sakakibara, H. Nakayama, and H. Misawa, Jpn. J. Appl. Phys., Part 1 **41**, 3015 (2002).
[18] M. Kikumoto, M. Kurachi, V. Tosa, and H. Tashiro, Biophys. J. **90**, 1687 (2006).
[19] Y. M. Sirenko, M. A. Stroscio, and K. W. Kim, Phys. Rev. E **53**, 1003 (1996).
[20] E. Nogales, M. Whittaker, R. A. Milligan, and K. H. Downing, Cell **96**, 79 (1999).
[21] V. VanBuren, D. J. Odde, and L. Cassimeris, Proc. Natl. Acad. Sci. U.S.A. **99**, 6035 (2002).
[22] A. Kis, S. Kasas, B. Babić, A. J. Kulik, W. Benoît, G. A. D. Briggs, C. Schönenberger, S. Catsicas, and L. Forró, Phys. Rev. Lett. **89**, 248101 (2002).
[23] S. Kasas, C. Cibert, A. Kis, P. D. L. Rios, B. M. Riederer, L. Forro, G. Dietler, and S. Catsicas, Biol. Cell **96**, 697 (2004).
[24] J. A. Tuszynski, T. Luchko, S. Portet, and J. M. Dixon, Eur. Phys. J. E **17**, 29 (2005).
[25] C. Q. Ru, *Elastic Models for Carbon Nanotubes, Encyclopedia of Nanoscience and Nanotechnology*, edited by H. S. Nalwa (American Scientific Publishers), 2004, Vol. 2, pp. 731–744.
[26] C. Y. Wang, C. Q. Ru, and A. J. Mioduchowski, J. Appl. Phys. **97**, 024310 (2005).
[27] C. Y. Wang, C. Q. Ru, and A. Mioduchowski, Phys. Rev. B **72**, 075414 (2005).
[28] W. Soedel, *Vibrations of Shells and Plates* (Marcel Dekker, New York, 1993).
[29] E. Ventsel and T. Krauthammer, *Thin Plates and Shells* (Marcel Dekker, New York, 2004).
[30] B. I. Yakobson, C. J. Brabec, and J. Bernholc, Phys. Rev. Lett. **76**, 2511 (1996).
[31] C. Q. Ru, Phys. Rev. B **62**, 9973 (2000).
[32] W. Flugge, *Stresses in Shells* (Springer-Verlag, Berlin, 1960).
[33] J. Schwaighofer and H. F. Microys, J. Appl. Mech. **46**, 356 (1979).
[34] R. D. Zou and C. G. Foster, Thin-Walled Struct. **22**, 143 (1995).
[35] X. Li and Y. J. Chen, Sound Vib. **257**, 967 (2002).
[36] A. Chajes, *Principles of Structural Stability Theory* (Prentice-Hall, Englewood Cliffs, NJ, 1974).
[37] S. O. Timoshenko and J. M Gere, *Theory of Elastic Stability* (McGraw-Hill, New York, 1961).
[38] F. Pamapaloni, G. Lattanzi, A. Jonas, T. Surrey, E. Frey, and E. L. Florin, Proc. Natl. Acad. Sci. U.S.A. **103**, 10248 (2006).
[39] C. Li, C. Q. Ru, and A. Mioduchowski, Biochem. Biophys. Res. Commun. **349**, 1145 (2006).
[40] E. Nogales and H. W. Wang, Curr. Opin. Cell Biol. **18**, 179 (2006).
[41] V. VanBuren, L. Cassimeris, and D. J. Odde, Biophys. J. **89**, 2911 (2005).